

FRACTURE ENERGY-BASED THERMODYNAMICALLY CONSISTENT GRADIENT MODEL FOR CONCRETE UNDER HIGH TEMPERATURE

GUILLERMO J. ETSE*[†], MARIANELA RIPANI* AND SONIA M. VRECH[†]

*CONICET, University of Buenos Aires
Av. Las Heras 2214, (C1127AAR) Buenos Aires, Argentina.
e-mail: getse@herrera.unt.edu.ar, mripani@fi.uba.ar

[†]CONICET, National University of Tucumán
Av. Roca 1800, (4000) Tucumán, Argentina.
e-mail: svrech@herrera.unt.edu.ar

Key words: Concrete, Gradient Plasticity, Thermodynamical Consistency, Fracture, Dehydration Degree, High Temperature

Abstract. Long term exposure to high temperature strongly affects the durability and safety of concrete structures due to the severe degradation process that takes place in this composite material. In effect, most of the relevant macroscopic mechanical features of porous materials like concrete such as cohesion, friction, strength, stiffness and ductility, strongly depend on the temperature, temperature gradient and humidity, as well as on the governing stress state. At the macroscopic level of observation, high temperature exposures cause significant modifications in the chemical features of cement paste. From the predictive analysis stand point, robust and reliable constitutive theories are required to accurately simulate the complex failure processes of concrete material subjected to high temperature exposure. In this work, a thermodynamically consistent gradient poroplastic theory for concrete under high temperature is proposed. Herein concrete is considered as a closed porous medium while the relevant thermo-chemo-mechanical couplings that take place in the material subjected to temperature effects are taken into account. Thereby, the dehydration of cement paste when is subjected to high temperature exposure is the main responsible for the degradation processes of fundamental mechanical properties. Regarding the gradient formulation a restricted form is considered whereby the state variables are the only ones of non-local character. A Temperature-Dependent Leon-Drucker-Prager (TD-LDP) strength criterion is proposed for porous material under high temperature fields and a numerical analysis by means of finite element simulations is presented to show the predictive capabilities of the proposed approach.

1 INTRODUCTION

Concrete exposures to high temperature may take place both in the case of accidents such as explosions or fire and under serviceability conditions such as furnaces structures, chimneys, kiln foundations, pressure vessels, etc. Concrete subjected to high temperature undergoes dramatic changes at microscopic level. One

of the most important is the cement paste dehydration that at macroscopic level results in stiffness and strength losses [1]. Actually, under temperature levels below 200°C, concrete shows no significant damage, because the resulting effects are only restricted to the evaporation of free water in the pores network. From 200°C starts the dehydration of the hydrated calcium silicates (CSH), essential components

that strongly contribute to the paste strength. Above 400°C takes place the calcium hydroxide (CH) dehydration and beyond 600°C also starts the rock aggregates degradation, being more vulnerable the siliceous than the calcareous ones, in terms of thermal damage. In this paper, the CSH dehydration is considered as the main concrete mechanical degradation cause. Therefore, high temperatures are understood as those that exceed 200°C. Then, water migration and water vapor through concrete pores processes are neglected. This means that the spalling on concrete surface due to the increasing pore pressure and thermal gradient is also neglected because this is a consequence of the water migration and water vapor dynamic processes. Accurate predictions of concrete failure behavior when subjected to high temperature require reliable theoretical frameworks, capable to more realistically reproduce the dramatic changes at microscopic levels by means of representative parameters. In this sense, the mechanics of continuum porous media, the thermodynamic laws and the concepts of non-local materials [2–6] define the most effective set of theoretical frames to approach this complex problem. Non-local effects in constitutive models lead also to objective predictions of post-peak behaviors regarding finite elements mesh density and orientation. On the other hand, they introduce a characteristic length which allows more accurate modeling of the pressure and thermal dependency of concrete failure processes in thermo-chemo-mechanical coupled problems.

The thermodynamically consistent formulation presented in this paper is based on a restricted gradient theory developed by Svedberg y Runesson [7] for the case of J_2 classical continuous media, expanded later by Vrech and Etse [8] for cohesive-frictional materials and recently by Mroginski et. al. [9] for porous media. This gradient theory assumes that a thermodynamic state for dissipative materials under isothermal processes is completely defined by the elastic strain and a finite number of internal softening/hardening plastic variables, being these latter the only of non-local charac-

ter. In this formulation, the dehydration degree, which is considered the controlling-parameter of the mechanical integrity, is incorporated as an additional internal variable, representing the chemical state. After presenting the fundamental equations of the proposed constitutive theory and model, the attention is focuses on the evaluation of this predictive capabilities.

2 PHYSICAL MODEL

Figure (1) shows the scheme of a representative volume of porous media. It is composed by the addition of two components: the solid skeleton particle and the fluid particle, both coincident in time and space. The solid skeleton is constituted by the solid matrix, the occluded porosity and the connected porosity. The fluid particle is composed of the fluids located in the connected porosity: water and air, according to the saturation condition [10].

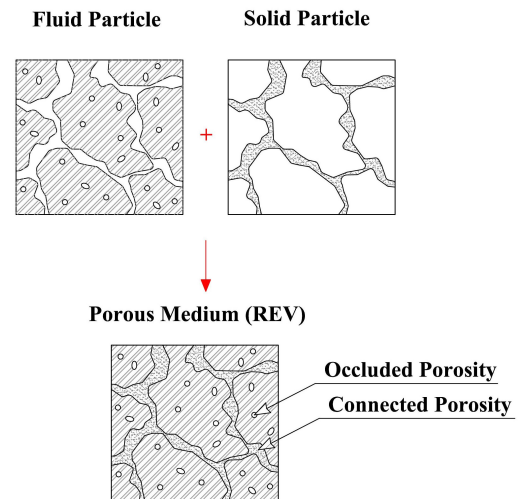


Figure 1: Porous Medium Composition.

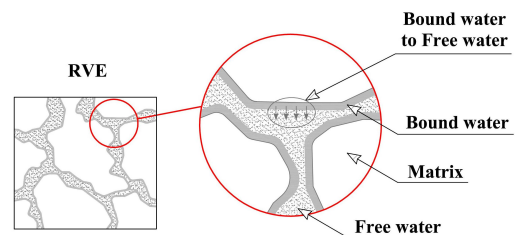


Figure 2: Dehydration Model.

2.1 DEHYDRATION MODEL

The calcium silicate hydrates (CSH) formation is the main responsible of the concrete mechanical strength development at early age [11], i.e. when the cement paste hydration process develops. Contrarily, in hardened concrete subjected to the action of high temperature, CSH undergoes a dehydration process which leads to the loss of material strength. Addressing the study of the concrete behavior as a porous medium, it is possible to consider the existence of bound water, chemically attached to the solid matrix and responsible for the integrity of the CSH. With increasing temperature the bound water becomes free, in this condition it leaves the solid skeleton and moves to the connected porosity, as shown in Fig.(2). This process is the main reason for the CSH dehydration and the degradation of concrete strength.

3 POROUS MEDIA THERMODYNAMICS

The first Thermodynamics law expresses the energy conservation, i.e. it defines the temporal balance between the internal energy, the kinetic energy, the mechanical work of external forces and the supplied heat

$$\dot{E} + \dot{K} = P_{ext} + Q^0; \quad E = \int_{\Omega} e d\Omega \quad (1)$$

The second Thermodynamics law states that the system energy can only irreversibly decrease

$$\dot{S} - Q_{\theta} \geq 0; \quad S = \int_{\Omega} s d\Omega \quad (2)$$

In the above equations, P_{ext} is the mechanical work done by external forces, Q^0 is the heat, E the system internal energy, S the system entropy, e the internal energy density, K the kinetic energy, Ω the volume, $\partial\Omega$ the surface boundary, $Q_{\theta} = Q^0/\theta$ the heat work per unit of absolute temperature θ , and s the entropy density.

The Clausius-Duhem inequality for open porous media takes the form, see Coussy, O. [12]

$$\int_{\Omega} \left[\boldsymbol{\sigma} : \dot{\boldsymbol{\varepsilon}} - g_m^{\beta} \nabla \cdot \mathbf{w}_{\beta} - s\dot{\theta} - \dot{\psi} + \right. \\ \left. - \mathbf{w}_{\beta} \cdot (\nabla g_m^{\beta} + s_m^{\beta} \nabla \theta) - \frac{\mathbf{h}}{\theta} \cdot \nabla \theta \right] d\Omega \geq 0 \quad (3)$$

where $\beta \in [1 : n]$ and n is the number of fluid components. Furthermore $\boldsymbol{\sigma}$ represents the second order Cauchy tensor, $\boldsymbol{\varepsilon}$ the second order absolute strain tensor, ψ the free Helmholtz energy, s_m the internal entropy per unit mass, \mathbf{w} a first order tensor corresponding to the fluid flux, g_m the enthalpy per unit flux mass and \mathbf{h} a first order tensor corresponding to the heat flux. In the above equations, $(\dot{\cdot})$ denotes the time derivative, and the bold letters represent tensors.

3.1 Chemo-mechanics of a closed porous medium

In this paper closed porous media are considered, i.e. there is no fluid exchange between the outside and the system. This implies that the fluid mass flow is null ($\mathbf{w}_{\beta} = 0$), therefore, the inequality given by Eq.(3) takes the form

$$\int_{\Omega} \left[\boldsymbol{\sigma} : \dot{\boldsymbol{\varepsilon}} - s\dot{\theta} - \dot{\psi} - \frac{\mathbf{h}}{\theta} \cdot \nabla \theta \right] d\Omega \geq 0 \quad (4)$$

Remark. Non-local analysis is based on the gradient plasticity theory, following the approach proposed by Svedberg, T. and Runesson, K., Vrech, S. M. and Etse, G. and Mroginski, J. et. al. [7–9], where the non-locality is limited to the internal state variables, adopted as scalar values. This proposal simplifies the study of non-local problem, respect to the approaches submitted by Gao, H. et. al., Fleck, N. A. and Hutchinson, J. W. and Gudmunson, P. [13–15].

$$\psi(\boldsymbol{\varepsilon}^e, \theta, \xi, \kappa, \nabla \kappa) = \psi^e(\boldsymbol{\varepsilon}^e, \theta, \xi) + \\ + \psi^{ch}(\xi) + \psi^{p,loc}(\xi, \kappa) + \psi^{p,nl}(\nabla \kappa) \quad (5)$$

Where ψ^e , ψ^{ch} , $\psi^{p,loc}$ and $\psi^{p,nl}$ represent the elastic, chemical, local plastic and gradient non-local contributions to the total free energy, respectively. Moreover, ε^e is the elastic component of the strain tensor, κ is a plastic internal state variable and ξ is the dehydration grade of the cement paste. From Eq.(5) follows the state equations

$$\boldsymbol{\sigma} = \frac{\partial \psi^e}{\partial \boldsymbol{\varepsilon}^e}; \quad S = -\frac{\partial \psi^e}{\partial \theta} \quad (6)$$

with the chemical, thermal and local plastic dissipations, D^{ch} , D^{th} and $D^{p,loc}$, respectively

$$\begin{aligned} D^{ch} &= -\frac{\partial \psi^{ch}}{\partial \xi} \dot{\xi} \geq 0; \\ D^{th} &= -\frac{\mathbf{h}}{\theta} \cdot \nabla \theta \geq 0; \\ D^{p,loc} &= \boldsymbol{\sigma} : \dot{\boldsymbol{\varepsilon}}^p - \frac{\partial \psi^{p,loc}}{\partial \kappa} \dot{\kappa} \geq 0 \end{aligned} \quad (7)$$

and the non-local plastic dissipation

$$\begin{aligned} D^{p,nl} &= \left(\nabla \cdot \frac{\partial \psi^{p,nl}}{\partial \nabla \kappa} \right) \dot{\kappa} + \\ &+ \int_{\partial \Omega} \mathbf{n} \cdot \frac{\partial \psi^{p,nl}}{\partial \nabla \kappa} \dot{\kappa} d\partial \Omega \geq 0 \end{aligned} \quad (8)$$

being $\boldsymbol{\varepsilon}^p$ the plastic component of the strain tensor and \mathbf{n} the normal vector to the boundary $\partial \Omega$. In a thermodynamically consistent chemo-gradient poroplastic system exists a convex set of admissible stress states fulfilling the following condition

$$\{(\boldsymbol{\sigma}, K, \xi) \mid F(\boldsymbol{\sigma}, K, \xi) \leq 0\} \rightarrow F(\boldsymbol{\sigma}, K, \xi) = f(\boldsymbol{\sigma}) - K(\lambda, \xi) = 0 \quad (9)$$

where K is the dissipative stress defined in terms of internal state variables and the dehydration degree, and λ a plastic multiplier. Furthermore, a dissipative potential can be defined as

$$Q(\boldsymbol{\sigma}, K, \xi) = g(\boldsymbol{\sigma}) - K(\lambda, \xi) = 0 \quad (10)$$

that fulfills the flow rule

$$\dot{\boldsymbol{\varepsilon}}^p = \frac{\partial Q}{\partial \boldsymbol{\sigma}} = \mathbf{m} \dot{\lambda}; \quad \dot{\kappa} = \frac{\partial Q}{\partial K} \dot{\lambda} \quad (11)$$

and the Kuhn-Tucker conditions

$$\dot{\lambda} \geq 0, \quad F(\boldsymbol{\sigma}, K, \xi) \leq 0, \quad \dot{\lambda} F(\boldsymbol{\sigma}, K, \xi) = 0 \quad (12)$$

with \mathbf{m} the plastic potential gradient

3.2 Constitutive Equations

In a closed porous medium, chemically reactive, each term of the free energy in Eq.(5) can be defined as follows

$$\begin{aligned} \psi^e &= \frac{1}{2} \boldsymbol{\varepsilon}^e : \mathbf{C} : \boldsymbol{\varepsilon}^e + \\ &- \theta \boldsymbol{\alpha} : \mathbf{C} : \boldsymbol{\varepsilon}^e + \frac{l}{\theta_0} \xi \theta - \frac{C}{2\theta_0} \theta^2 \end{aligned} \quad (13)$$

$$\begin{aligned} \psi^{ch} &= \frac{h^{ch}}{2} \xi^2 - A_0 \xi; \\ \psi^{p,loc} &= -\frac{1}{2} h(\xi)^{loc} \kappa^2 \\ \psi^{p,nl} &= \frac{1}{2} l_c^2 H^g \nabla \cdot \nabla \kappa \end{aligned} \quad (14)$$

Thereby is C the concrete heat capacity, h^{loc} the softening/hardening chemo-plastic modulus, A_0 the initial chemical affinity, l_c the gradient characteristic length, H^g the softening/hardening gradient modulus, θ the temperature, l the latent dehydration heat, h^{ch} the chemical modulus and $\boldsymbol{\alpha} = \alpha \mathbf{II}$, with α the concrete thermal dilatation coefficient and \mathbf{II} the second order identity tensor. From Eqs.(7) and (8), the dissipative stresses $K^{ch} = -\partial \psi^{ch} / \partial \xi$, $K^{p,loc} = -\partial \psi^{p,loc} / \partial \kappa$ and $K^{p,nl} = \nabla \cdot \partial \psi^{p,nl} / \partial \nabla \kappa$ are obtained, while from Eq.(6) the total and dissipative stresses

$$\begin{aligned} \dot{\boldsymbol{\sigma}} &= \mathbf{C} : \dot{\boldsymbol{\varepsilon}}^e + \alpha \mathbf{I} : \mathbf{C} \dot{\theta}; \\ \dot{S} &= \frac{C}{\theta_0} \dot{\theta} + \frac{l}{\theta_0} \dot{\xi} \end{aligned} \quad (15)$$

are derived. Finally, from Eqs.(13) and (14) follows

$$\begin{aligned}\dot{K}^{p,loc} &= -h(\xi)^{loc}\dot{\kappa} - \frac{\partial h(\xi)^{loc}}{\partial \xi} \frac{\kappa^2}{2} \dot{\xi} \\ \dot{K}^{ch} &= -h^{ch}\dot{\xi} + \frac{l}{\theta_0} \dot{\theta}\end{aligned}\quad (16)$$

$$\dot{K}^{p,nl} = -l_c \nabla \cdot (H^g \nabla \kappa) \quad (17)$$

The coefficients in Eqs.(15), (16) and (17) are achieved from the Helmholtz free energy, resulting

$$\begin{aligned}\mathbf{C} &= \frac{\partial^2 \psi^e}{\partial \boldsymbol{\varepsilon}^e \partial \boldsymbol{\varepsilon}^e}; \quad \alpha \mathbf{I} : \mathbf{C} = \frac{\partial^2 \psi^e}{\partial \boldsymbol{\varepsilon}^e \partial \theta} \\ \frac{C}{\theta_0} &= \frac{\partial^2 \psi^e}{\partial \theta \partial \theta}; \quad \frac{l}{\theta_0} = \frac{\partial^2 \psi^e}{\partial \theta \partial \xi}\end{aligned}\quad (18)$$

$$h(\xi)^{loc} = -\frac{\partial^2 \psi^{p,loc}}{\partial \kappa \partial \kappa} \quad h^{ch} = \frac{\partial^2 \psi^{ch}}{\partial \xi \partial \xi} \quad (19)$$

$$H^g = \frac{1}{l_c^2} \frac{\partial^2 \psi^{p,nl}}{\partial \nabla \kappa \partial \nabla \kappa}; \quad (20)$$

4 THERMAL BALANCE AND KINETICS OF DEHYDRATION

From Eqs.(2) and (15-b), and assuming the Fourier law for the temperature distribution ($\mathbf{h} = -k \nabla \theta$) the heat equation that determines the temperature distribution in space and time is achieved

$$C \dot{\theta} = k \nabla \cdot \nabla \theta + l \dot{\xi} \quad (21)$$

where k represents the concrete heat conductivity. Moreover, for determining the dehydration degree depending on the applied temperature, it is necessary to evaluate Eq.(16-b) when $K^{ch} \rightarrow 0$. According to the experimental evidence, each temperature level can be linearly and uniquely related to the cement paste dehydration level [1]. Therefore, the following function can be considered

$$\xi = \gamma(\theta - 20) \quad (22)$$

with θ in Celsius degrees and $\gamma = 0.0015$.

5 CONSTITUTIVE MODEL

To model and predict the response of concrete in the framework of a thermodynamically-consistent gradient-elastoplastic theory, the Temperature-Dependent Leon-Drucker-Prager Criterion (TD-LDP) is proposed, that arises from the reformulation of the Leon Drucker-Prager (LDP) failure criterion [16]. The TD-LDP failure surface is given in Eq.(23) and its isotropic variation with different dehydration levels is shown in Fig.(3).

$$F^*(\rho, p, \xi) = \frac{3}{2} \rho^* + m \left(\frac{\rho^*}{\sqrt{6}} + p^* \right) - (1 - \xi) = 0 \quad (23)$$

where

$$\begin{aligned}p^* &= \frac{p}{f'_c}; \quad \rho^* = \frac{\rho}{f'_c} \\ \rho &= \sqrt{2J_2}; \quad p = \frac{tr \boldsymbol{\sigma}}{3}\end{aligned}\quad (24)$$

with p and ρ , the deviatoric and volumetric coordinates in the Haigh Westergaard stress space, and f'_c and f'_t the maximum compressive and tensile strengths, respectively and J_2 the second invariant of deviatoric stresses, while the friction parameter has the following expression

$$m = \frac{3}{2} \frac{f'_c{}^2 - f'_t{}^2}{f'_c f'_t} \quad (25)$$

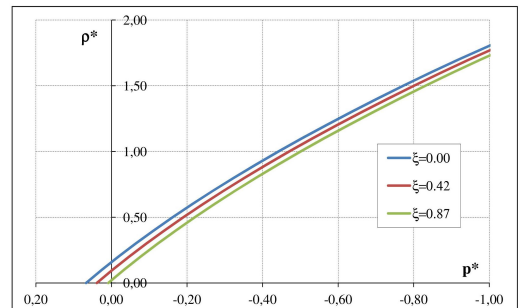


Figure 3: TD-LDP Model Failure Surfaces.

Beyond the elastic regime, plastic strains take place and the material exhibit hardening or

softening. To capture these behaviors a yield surface is proposed

$$F(\rho^*, p^*, K_h, K_s) = \frac{3}{2}(\rho^*)^2 + K_h m \left(\frac{\rho^*}{\sqrt{6}} + p^* \right) - (1 - \xi) K_h K_s = 0 \quad (26)$$

Furthermore, a potential surface is adopted to reduce the excessive plastic volumetric strains

$$Q(\rho^*, p^*, K_h, K_s) = \frac{3}{2}(\rho^*)^2 + K_h m \left(\frac{\rho^*}{\sqrt{6}} + \eta p^* \right) - (1 - \xi) K_h K_s = 0 \quad (27)$$

with η the non-associative variable, K_h and K_s defined as follows

$$K_h = 0.1 + 0.9 \sin \left[\frac{\pi}{2} \frac{\|\mathbf{m}\| \lambda}{x_p(p^*, \xi)} \right] \quad (28)$$

$$K_s = K_s^f(\kappa, \xi) + K_s^g(\nabla \kappa) \\ K_s = \exp \left[-5 \frac{h_t(\xi)}{R_G(p^*)} \frac{\|\langle \mathbf{m} \rangle\| \lambda}{u_r} \right] + -l_c^2 H^g \nabla^2 \kappa \quad (29)$$

In the above equations, $x_p(p^*, \xi)$ represents the plastic strain corresponding to the peak load. It can be interpreted as a hardening ductility measure, depending on the pressure confinement and the dehydration degree. In Eq.(29) K_s^f represents the stiffness degradation due to macro or micro-cracking processes, K_s^g is the decohesion of the solid between cracks and u_r denotes the maximum crack opening, while $h_t(\xi)$ the total continuum height depending on the dehydration degree. The Mc. Cauley brackets are defined as $\langle x \rangle = 0.5(x + |x|)$. R_G is the ratio between G_f^{II} and G_f^I and it remains constant with temperature variations. The gradient contribution to the material stiffness and softening is defined

by K_s which is a function of the characteristic length l_c . The last one is defined in terms of the acting confinement pressure. The functions of x_p , $h_t(\xi)$ and R_G are expressed as

$$x_p(p^*, \xi) = A_h \exp [B_h p^* + C_h \xi] \quad (30)$$

$$h_t(\xi) = h_t (A_s \xi^2 - B_s \xi + C_s) \quad (31)$$

$$R_G(p^*) = \begin{cases} 1 & p^* \geq 0, \\ C_u + D_u \sin \left(2p^* - \frac{\pi}{2} \right) & -1.5 \geq p^* \leq 0, \\ 100 & p^* \leq -1.5. \end{cases} \quad (32)$$

where A_h , B_h , C_h , A_s , B_s are constants to be calibrated from experimental results, $C_s = 1.00$ and h_t is the total continuum height at room temperature. The variation of R_G in terms of p^* and $h_t(\xi)$ in terms of ξ are shown in Figs.(4) and (5), respectively.

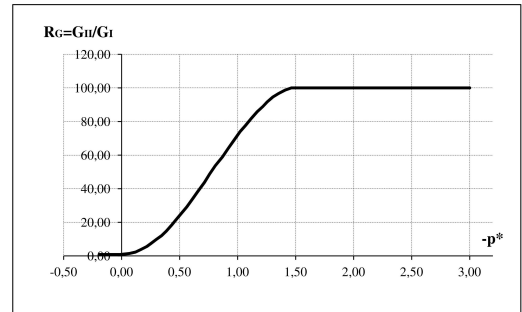


Figure 4: Variation of R_G in terms of the confinement pressure [8]

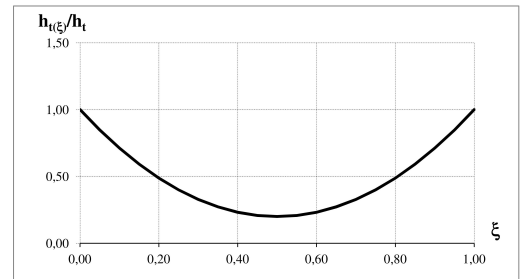


Figure 5: Variation of R_G in terms of the dehydration degree

6 THERMODYNAMICAL CONSISTENCY OF THE TD-LPD MODEL

The plastic energies in hardening and softening regimes of the proposed model can be expressed as

$$\psi_h^p(\kappa, \xi) = -0.1\kappa - \frac{0.9}{\kappa} \cos(-\alpha_h \kappa) \quad (33)$$

$$\psi_s^p(\kappa, \xi, \nabla \kappa) = -\frac{1}{\alpha_s} \exp(\alpha_s \kappa) + \frac{1}{2} l_c^2 H^g \nabla \cdot \nabla \kappa \quad (34)$$

respectively, where

$$\alpha_h = \frac{\pi}{2} \frac{\|m\| \lambda}{x_p(1 - \xi)} \quad (35)$$

$$\alpha_s = \frac{5h_t}{u_r R_G(p^*)} \frac{\|m\| \lambda}{(1 - \xi)} \quad (36)$$

Taking into account Eqs.(7-c) and (8) and the above expressions for the plastic energies, then Eqs.(28) and (29) for the dissipative stresses K_h and K_s can be obtained and the fulfillment of the thermodynamical consistency is demonstrated.

7 RESULTS

In this section, the numerical predictions of the model for the uniaxial compression test considering uniform temperature profile is presented. The numerical implementation considers a mixed constant strain triangular FE for gradient plasticity [17] under axialsymmetric conditions. A quarter of the real specimen (7.5cm x 15cm), was analyzed due to the double symmetry conditions, using a uniform mesh of 384 elements, see Fig.(6).

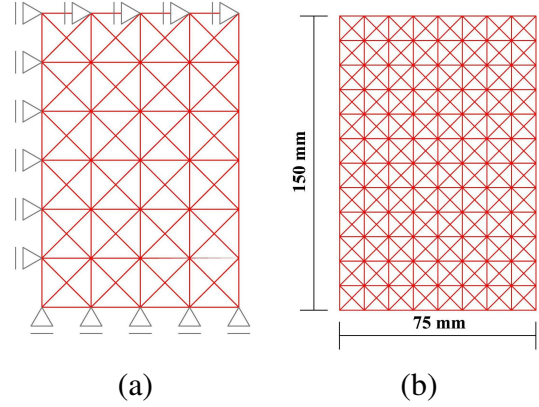


Figure 6: (a) Boundary conditions; (b) FE discretization.

For the stiffness degradation a linear relationship was considered in the form $E = E_0(1 - \xi)$, see Ulm, F. J. and Coussy, O. [1], being E_0 the elasticity modulus of the non-degraded concrete. The considered materials properties are shown in Table (1) while the model parameters are summarized in Table (2).

Table 1: Concrete Properties

Elasticity Modulus - E_0	19300	MPa
Poisson Modulus - ν	0.20	-
Compressive Strength - f'_c	22.00	MPa
Tensile Strength - f'_t	2.20	MPa
Maximum Crack Opening - u_r	0.127	mm
Sep. between Tens. Cracks - h_t	108.00	mm
Internal Length - l_c	30.00	mm
Gradient Modulus - H^g	1.00	MPa

Table 2: Model Parameters

A_h	0.0007
B_h	-0.0089
C_h	4.50
$R_G(p^*)$	4.60
A_s	3.20
B_s	3.20
C_s	1.00

Figure (7) depicts the predicted total plastic strain profile for the inhomogeneous compression test when the concrete probe is subjected

to 300°C, whereas Fig.(8) illustrates the same results when the applied temperature is 500°C.

The results of the stress-strain curves in compression tests for different dehydration levels are shown in Fig.(9) and compared with the experimental stress-strain curve at environment temperature proposed by Hurbult, B. [18] for the same concrete. It could be clearly observed the decrease of the stiffness and the peak strength with increasing temperature due to increase of the dehydration degree. Furthermore, an increase in the fracture energy can be evidenced, this trend continues until around 400°C, starting to decrease from that temperature. These results are in agreement with experimental data carried out by Lee et. al. [19] shown in Fig.(10).

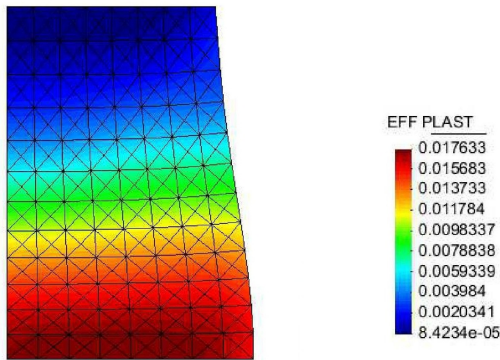


Figure 7: Plastic strain distribution in Uniaxial Compression test with inhomogeneous vinculation after 300°C exposure.

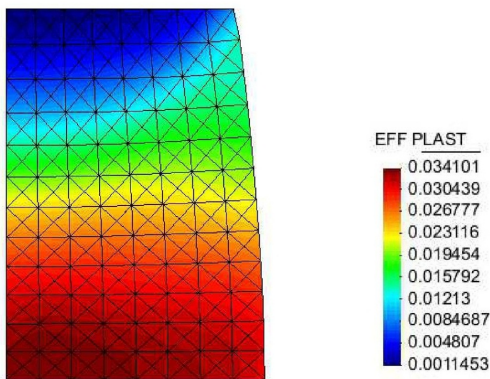


Figure 8: Plastic strain distribution in Uniaxial Compression test with inhomogeneous vinculation after 500°C exposure.

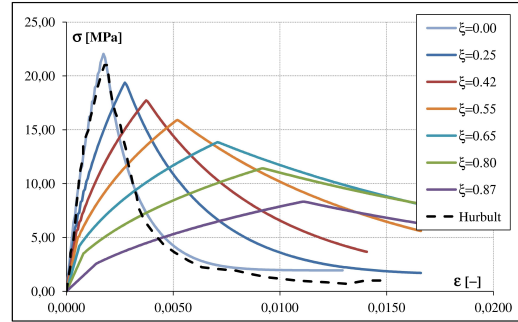


Figure 9: Uniaxial Compression test of normal concrete (22.50MPa) after high temperatures.

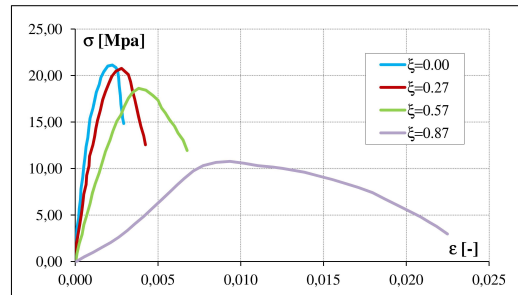


Figure 10: Experimental Uniaxial Compression tests on Normal Concrete (27.60MPa) after High Temperature exposures.

7.1 Future Developments

Presently, the authors are working in the calibration of the gradient characteristic length in terms of the dehydration degree.

8 CONCLUSIONS

In this work a thermodynamically consistent gradient poroplastic model for concrete subjected to high temperature is proposed. The model takes into account the thermo-chemo-mechanical coupling in porous materials like concrete when they are considered as non-local closed porous media. The controlling parameter is the dehydration of cement paste when subjected to high temperature exposure. A particular form of gradient poroplasticity is considered whereby the state variables are the only ones of non-local characters. The post-peak behavior is defined by a combined mechanism of fracture energy release-based softening process in the active micro-cracks, and a gradient-based softening in the solid material in between cracks.

Thereby, the gradient characteristic length is defined in terms of the acting confining pressure while the fracture energy characteristic length is defined in terms of both the confining pressure and the dehydration degree. The proposed model is able to realistically and objectively predict the temperature dependent failure behavior of concrete. Particularly, the model is capable to reproduce the variation of strength, stiffness and post-peak ductility in terms of the acting temperature.

9 ACKNOWLEDGEMENTS

The authors acknowledge the financial support for this work by CONICET (National Council for Science and Technology) through the Grant PIP 112-200801-00707 and by CIUNT (Research Council of the University of Tucuman) through the Grant 26/E479.

REFERENCES

- [1] Ulm, F. J. and Coussy, O., 1999. The Chunnel Fire I: Chemoplastic softening in rapidly heated concrete. *J. Eng. Mech.-ASCE* **125**:272–289.
- [2] Zbib, H. M., and Aifantis, E. C., 1988. On the localization and postlocalization behavior of plastic deformation. *III, Res. Mechanica*. **23**:261–305.
- [3] Etse G. and Willam, K., 1994. Fracture energy formulation for inelastic behavior of plain concrete. *J. Eng. Mech.* **120**:1983–2011.
- [4] Etse G., and Steinmann, P., and Nieto M., 2003. A micropolar microplane theory. *Int. J. Eng. Sci.* **41**:1631–1648.
- [5] Etse G. and Vrech S., 2006. Geometrical method for localization analysis in gradient-dependent J_2 plasticity. *J. Appl. Mech.* **73**:1026–1030.
- [6] Abu Al-Rub R. K. and Voyiadjis G. Z., 2006. A physically based gradient plasticity theory. *Int. J. Plasticity* **22**:654–684.
- [7] Svedberg, T. and Runesson, K., 1997. A thermodynamically consistent theory of gradient-regularized plasticity coupled to Damage. *Int. J. Plasticity*. **13**:669–696.
- [8] Vrech, S. and Etse, G., 2009. Gradient and fracture energy-based plasticity theory for quasi-brittle materials like concrete. *Comput. Meth. Appl. Mech.* **199**:136–147.
- [9] Mroghinski, J. and Etse, G. and Vrech, S., 2010. A thermodynamical gradient theory for deformation and strain localization of porous media. *Int. J. Plasticity*. **27**:620–634.
- [10] Coussy, O., 2004. *Poromechanics*. John Wiley & Sons.
- [11] Ulm, F. J. and Coussy, O., 1995. Modeling of thermochemomechanical couplings of concrete at early ages. *J. Eng. Mech.-ASCE*. **121**:785–794.
- [12] Coussy, O., 1995. *Mechanics of Porous Continua*. John Wiley & Sons.
- [13] Gao, H and Huang, Y and Nix, W. D. and Hutchinson, J. W., 1999. Mechanism-based strain gradient plasticity I. Theory. *J Mech Phys Solids*. **47**:1239–1263.
- [14] Fleck, N. A. and Hutchinson, J. W., 2001. A reformulation of strain gradient plasticity. *J Mech Phys Solids*. **49**:2245–2271.
- [15] Gudmunson, P., 2004. A unified treatment of strain gradient plasticity. *J Mech Phys Solids*. **52**:1379–1406.
- [16] Vrech, S. M., 2007. Computational simulation of localized failure process based on gradient theory (in spanish). *PhD. Thesis*. National University of Tucuman, Argentine.
- [17] Svedberg, T., 1999. On the modelling and numerics of gradient-regularized plasticity coupled to damage. *PhD. Thesis*. Chalmers University of Technology, Sweden.

- [18] Hurbult, B., 1985. Experimental and computational investigation of strain-softening in concrete. *Master Thesis*. University of Colorado.
- [19] Lee, J. and Xi, Y. and Willam, K., 2008. Properties of concrete after high-temperature heating and cooling. *ACI Mater. J.* **105**:334–341.